European Journal of Pharmaceutical Sciences 155 (2020) 105542

Contents lists available at ScienceDirect

European Journal of Pharmaceutical Sciences

journal homepage: www.elsevier.com/locate/ejps

A new drug testing platform based on 3D tri-culture in lab-on-a-chip devices

Begum Gokce[a], Ismail Akcok[b], Ali Cagir[b], Devrim Pesen-Okvur[c,*]

[a] Izmir Institute of Technology, Biotechnology and Bioengineering Graduate Program, Turkey
[b] Izmir Institute of Technology, Department of Chemistry, Turkey
[c] Izmir Institute of Technology, Department of Molecular Biology and Genetics, Turkey

ARTICLE INFO

Keywords:
Drug discovery
Breast cancer cell
3D cell culture
Tri-culture, doxorubicin
(R)-4′-methylklavuzon
Lab-on-a-chip

ABSTRACT

Drug discovery has a 90% rate of failure because preclinical platforms for drug testing do not mimic the *in vivo* conditions. Doxorubicin (DOX) is a commonly used drug to treat breast cancer patients even though it has side effects. Lab-on-a-chip (LOC) devices provide spatial control at the micrometer scale and can thus emulate the cancer microenvironment. Here, using a multidisciplinary approach, a new drug testing platform based on 3D tri-culture in LOC devices was developed. Breast cancer cells alone or with normal mammary epithelial cells and macrophages were cultured in matrigel in LOC devices. The platform was used to test DOX and (*R*)-4′-methylklavuzon (KLA), which is a new anti-cancer drug candidate. Results showed that DOX and KLA were equally effective on breast cancer cells in 3D monoculture. KLA produced 26% less death for breast cancer cells than DOX in 3D tri-culture. More importantly, DOX was not selective between breast cancer cells and normal mammary epithelial cells in 3D tri- culture whereas KLA caused 56% less cell death than DOX for normal mammary epithelial cells. Results strongly recommend that 3D tri-culture in LOC devices be used for assessment of drug toxicity at the preclinical stage.

1. Introduction

A critical problem in the development of effective disease treatments is the lack of adequate model systems to identify drug targets, screen toxicity, and predict clinical drug efficacy. Traditional animal models or conventional cell cultures do not accurately mimic human physiology, and thus tend to fail to recapitulate diseases and to predict human responses to medical treatments. This is a major cause of drug development failures late in clinical trials, resulting in expensive new drugs, and lack of medication for some diseases. In addition, ethical questions raised by animal use increase the pressure to minimize animal experimentation. For these reasons, the pharmaceutical industry is looking for new ways to improve the drug development process.

Pharmaceutical companies spend a tremendous amount of money on research and development each year, reaching nearly $179B worldwide in 2018 (Waters, 2019). The drug discovery process can take 12–15 years from the discovery stage to FDA approval. A cancer drug can cost $2.6B. Discovery and pre-clinical stages together constitute approximately 30 % of the total cost and time period of the whole process (Woodcock and Woosley, 2008; Alterovitz et al., 2018; Schuhmacher and Gassmann, et al. 2018).

Doxorubicin (DOX), extracted from *Streptomyces peucetius* var. *caesius,* is a fluorescent anthracycline antibiotic derivative (Arcamone et al., 1969). DOX has been considered as one of the most effective agents against breast cancer (Brenner and Brenner, 1983; Namer, 1993). The mechanism of action of DOX has been previously studied (Keizer et al., 1990; Wang, et al., 2004, 2006, Tacar et al., 2013). Goniothalamin, which is isolated from *Goniothalamus macrophyllus*, is a component with selective cytotoxic properties against cancer cells. Kasaplar et. al., modified the structure of goniothalamin and synthesized a new molecule, a naphthalen-1-yl substituted α,β-unsaturated-δ-lactone derivative and named it (*R*)-4′-methylklavuzon (KLA), which has increased cytotoxic activity compared to the parent molecule (Kasaplar et al., 2009, Tacar et al., 2015, Akcok, et al., 2017, Kanbur et al., 2017). The mechanism of action of KLA has also been previously studied (Akcok et al., 2017; Delman et al., 2019). The mechanism of action of both molecules, DOX and KLA, involves more than one intracellular target. DOX can act through DNA intercalation, Topo II inhibition and histone eviction. KLA can cause cell death by inhibition of CRM1, Topo I and SIRT I enzymes. What is more important is that the exhibition of inhibition is different at the molecular level: DOX is a reversible inhibitor and its reversible interaction with the surrounding totally occurs by physical attractive and repulsive forces. On the other hand, KLA is an irreversible inhibitor. It can make covalent bonds with the nucleophilic parts of the macromolecules, including the proteins of matrigel. Therefore, a new drug testing platform should be

* Corresponding author.
E-mail address: devrimpesen@iyte.edu.tr (D. Pesen-Okvur).

https://doi.org/10.1016/j.ejps.2020.105542
Received 29 May 2020; Received in revised form 10 July 2020; Accepted 2 September 2020
Available online 12 September 2020

tested with both reversible and irreversible inhibitors. DOX is a very well-studied drug and is used in the clinic despite its known toxicity. Here DOX was chosen as the reference drug. The new drug candidate, KLA, was also tested.

A tumor in the human body is not comprised of cancer cells in a monolayer. First of all, a 3D setting exists. Cancer cells are also not in void, but exist in a scaffold of extracellular matrix. In addition, the tumor microenvironment is composed of many different cell types including cancer cells, normal epithelial cells, fibroblasts, immune cells, etc. (Ma et al., 2010). In order to obtain clinically relevant results in drug testing, the microenvironment of the test platform should mimic the *in vivo* conditions as best as possible (Miki et al., 2012). 3D cell culture has already proven to be superior to 2D cell culture by many studies. (Cukierman et al. 2001; Shield et al., 2009; Hirschhaeuser et al., 2010; Edmondson et al., 2014). These studies show that morphology, proliferation, exposure to medium/drugs, stage of cell cycle, gene/protein expression and drug sensitivity are closer between 3D culture systems and the in vivo conditions than that of 2D culture systems. For example, drugs that appear effective in 2D turn out to be less effective in 3D. What is more, presence of non-cancer cells has also been shown to affect results of drug tests even in 2D cell culture (Goers et al., 2014; Imamura et al., 2015; Duval et al., 2017; Kasurinen et al., 2018). Furthermore, a test platform that can faithfully mimic the *in vivo* condition in human tissues will significantly reduce animal testing (Amelian et al., 2017).

Microfluidic or lab-on-a-chip (LOC) devices are increasingly being used in pharmaceutical and life sciences (Wielhouwer et al., 2011; Ziolkowska et al., 2011; Farooq et al., 2019; Oliveira et al., 2019; Khajuria et al., 2020). LOC devices aimed at cellular studies require only a few microliters of culture medium or cells suspended in culture medium or cells mixed with a matrix or drugs diluted to their working concentrations, and thus reduce both reagent consumption and waste generation. LOC devices are portable, low cost, disposable and thus are well suited for high throughput, industrially scalable assays. More importantly, LOC devices provide spatial and temporal control, which is translated into fabrication of physiologically relevant microenvironments (Huh et al., 2011; Bhatia and Ingber, 2014; Popova et al., 2015). LOC devices can play various critical roles in the early detection, diagnosis and treatment of cancer patients (Barata et al., 2016) and are especially well suited for the preclinical stages of the drug discovery process.

Mimicking a tumor perfectly *in vitro* is still ongoing work. Here we aimed to mimic the dimensionality and the cellular diversity to move away from a 2D cancer cell monolayer model and closer to a real tumor. The platform developed in this work is based on previous literature that shows (1) cellular response to drugs in 3D is more relevant to the in vivo response when compared with the cellular response in 2D; (2) cellular response to drugs in the presence of multiple cell types is more relevant to the *in vivo* response when compared with the cellular response in mono-cultures. Here, the focus is on the assessment of the toxicity of drugs by examining cell death. Such an assessment is indispensable in the preclinical stage and provides preliminary data for the clinical stage. When the assessment of toxicity is performed in a setting that is relevant to the *in vivo* conditions as much as possible, better selected candidate drugs can be forwarded to the animal and clinical studies.

2. Materials and methods

MDA-MB-231, MCF10A and RAW264.7 cells were obtained from ATCC (LGC Standards, Germany). Cell culture materials were purchased from Biological Industries (Israel). Doxorubicin (DOX) and media supplements were acquired from Sigma Aldrich (Germany). Dextran Alexa Fluor 488; 10 kDa (Cat No: D22910), Dextran Alexa Fluor 680; 3 kDa (Cat No: D34681), CellTracker Green CMFDA Dye (Cat No: C2925), CellTracker Blue Dye (Cat No: C2110) and NucRed Dead 647 Reagent (Cat No: R37113) were obtained from ThermoFisher Scientific (USA). PDMS elastomer base and curing agent were purchased from SYLGARD Dow Corning (USA).

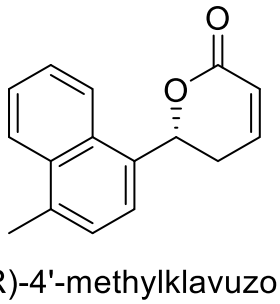

Fig. 1. Chemical structure of (*R*)-4′-methylklavuzon (KLA).

2.1. (R)-4′-Methylklavuzon synthesis

(*R*)-4′-methylklavuzon (Klavuzon) was synthesized through a three-step procedure starting from 4-methyl-1-naphthaldehyde as described in the literature (Delman et al., 2019). The synthesis started with the asymmetric allylation of 4-methyl-1-naphthaldehyde by addition of allyltrimethoxysilane in the presence of (*R*)-Tol-BINAP.AgF catalyst (Yanagisawa et al., 1999). Afterwards, produced chiral homoallylic alcohol was converted to acrylate ester by addition of acryloyl chloride under basic condition. Ring closing metathesis reaction of acrylate ester with 1st generation Grubbs' catalyst yielded (*R*)-4′-methylklavuzon (Fig. 1).

2.2. Cell culture

MDA-MB-231 (breast cancer, triple negative, invasive) cells were cultured in DMEM High Glucose supplemented with 10% fetal bovine serum (FBS), 1% pen-streptomycin and 1% L-glutamine. MCF-10A (normal mammary epithelial) cells were cultured in DMEM/F-12 supplemented with 5% donor horse serum, 20 ng/ml EGF, 0.5 μg/ml hydrocortisone, 100 ng/ml cholera toxin and 10 μg/ml insulin. RAW 264.7 (macrophage) cells were cultured in RPMI1640 supplemented with 10% FBS, 1% pen-streptomycin, 1% L-glutamine. Cells were incubated at 37 °C with 5 % CO_2.

2.3. Fabrication of lab-on-a-chip (LOC) devices

The LOC devices were fabricated as described previously (Ozdil et al., 2014). Briefly, SU-8 molds were prepared by UV lithography. SU-8 molds were used for casting PDMS structures. PDMS structures were bonded with glass surfaces after UV/ozone treatment. The LOC devices were sterilized by UV light before cell culture experiments. The LOC device had three parallel channels separated by a series of trapezoid posts (Fig. 2) that acted as capillary burst valves (Yildirim et al., 2014) which made it possible to load a matrix into the middle channel without leakage into the side channels. Having a series of posts instead of a solid wall between channels also allowed molecules to move between channels. The width of the middle channel was not constant due to the trapezoid shapes of the posts: The minimum and maximum widths of the middle channel were 1 and 2 mm. The widths of the side channels were 2 mm. The heights of all channels were ~ 295 μm. Lengths of channels were 8 mm. Fig. 2 shows the LOC device used and the experimental set-up. Please also refer to Supplementary Data Movie 1 that shows loading of green colored water into a LOC device.

2.4. Diffusion in LOC devices

Diffusion in LOC devices was determined by fluorescence time lapse

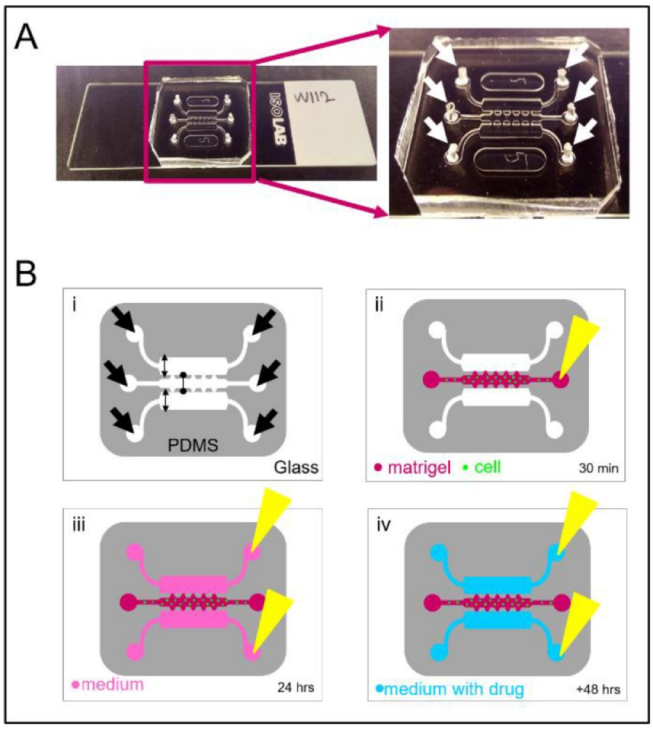

Fig. 2. LOC and experimental set-up. (A) Photograph of LOC fabricated on a standard microscope slide. (B) Experimental set-up (i) Empty LOC. Lines ending in arrows showed the widths of the side channels while line ending in points showed the width of the middle channel. (ii) The middle channel of LOC was loaded with cell-laden matrigel, which polymerized after 30 min. (iii) Side channels of LOC were loaded with medium and incubated for 24 h (iv) Media in side channels of LOC were changed with drug containing medium and incubated for another 48 h. White and black lines with arrows show the inlet and outlet ports. Yellow triangle represents a 20 μl pipet tip.

imaging. Matrigel was diluted to 4 mg/ml with culture medium, loaded into the matrix channel and the LOC devices were incubated at 37 °C for 30 min for matrigel polymerization. Fluorescently labeled 3 and 10 kDa dextran molecules were loaded into one of the side channels of the chip. Final concentration of both of the dextran molecules was 0.1 mg/ml. Culture medium was loaded into the other side channel. Images were taken with a Leica SP8 confocal microscope with 5X magnification every 5 min for a total of 60 min. Signals were detected in green and far red channels with laser excitations at 488 and 638 nm and emission windows of 500–540 and 650–780 nm. Images were analyzed with ImageJ/Fiji. Permeability coefficients were calculated as described previously (van Duinen et al., 2017).

2.5. Cell culture in LOC devices

MDA-MB-231 and MCF10A cells were stained with CellTracker Green and CellTracker Blue dyes, respectively, one day before being loaded onto the LOC devices. Cells were processed for passaging, re-suspended in medium and mixed with matrigel (8 mg/ml) at a 1:1 ratio and loaded into the middle channel. Both the mixture and the LOC devices were kept on ice before and during loading. Cell-laden matrigel loaded LOC devices were kept at 37 °C with 5 % CO_2 for 30 min to allow for the polymerization of the matrigel. Culture medium used for MDA-MB-231 cells was loaded into the side channels for both mono- and tri-culture experiments. MDA-MB-231 cells were used for mono-culture. MDA-MB-231, MCF-10A and RAW 264.7 cells were used at 1:1:1 ratio for tri-culture. Final total cell density in LOC devices was 10 x 10^6 cells/ml for all experiments. LOC devices were placed in sterile petri dishes housing pieces of autoclaved filter paper wetted with sterile H_2O to help prevent polymerization.

2.6. Drug treatment

After 24 h in culture, media in the side channels of LOC devices were replenished with culture media containing DMSO, DOX or (*R*)-4′-methylklavuzon. DMSO was used as a solvent for both drugs. Final concentrations of DOX and (*R*)-4′-methylklavuzon were 10 μM and 100 μM in the LOC devices, respectively. The LOC devices were kept in culture for another 48 h.

2.7. Cell viability assessment via 3D imaging

After a total of 72 h in culture, NucRed Dead 647 reagent was added to the side channels of LOC devices and incubated for 1 h. Z-stack images of the cell-laden matrigel containing middle channels of the LOC devices were acquired using a Leica SP8 Confocal microscope at 10X magnification. Excitation laser and emission window wavelengths for blue, green, red and far-red channels were 405, 488, 552, 638; 410–507, 493–556, 557–634, 643–776 nm, respectively. Blue, green, red and far-red channels correspondingly showed MCF10A cells, MDA-MB-231 cells, DOX and all dead cells.

2.8. Image analysis

ImageJ/Fiji was used for image analysis (Schneider et al., 2012) (Schindelin et al., 2012). Apparent volumetric occupancy was calculated from area fractions of selected regions of interest in the top views of 3D images. For death index analysis, a custom in-house written macro was used. Here, Z-stack images were converted to sum projections and thresholded. The death index for each cell type was defined as the ratio of the number of pixels that were positive for both signal1 and signal2, to the number of pixels that were positive for signal1. Signal1 was the raw integrated fluorescent signal from cells of interest and signal2 was the raw integrated fluorescent signal from all dead cells.

2.9. Statistical analysis

For all experiments, at least three biological and three technical independent experiments were performed. The data were expressed as a mean ± s.e.m. Student's *t*-test was used for statistical analysis. A p value of <0.05 was considered significant.

3. Results and discussion

3.1. Determination of diffusion profiles in LOC devices

To ensure that culture medium components and drugs to be added to the side channels of the LOC devices can efficiently reach the cells in the middle channel, the diffusion profiles of 3 and 10 kDa fluorescent dextran molecules in the LOC devices (Fig. 3) were determined. The middle channel was loaded with cell-free matrigel. After polymerization of matrigel was complete, one of the side channels of the LOC device was loaded with culture medium containing fluorescent dextran molecules while the other side channel was loaded with culture medium only. The bright areas in the images showed the fluorescence signal of the dextran molecules. Both dextran molecules showed diffusion from the side channel they were loaded into to the middle channel with matrigel. As expected, the diffusion was faster when the molecular weight of the dextran was smaller. 3 kDa dextran crossed over the whole middle channel before the 10 kDa dextran (Fig. 3A, 3B). The dashed line along the border of the source channel and the matrigel showed the position for examining the distribution of fluorescence intensities. A representative intensity profile for the 0 and 60 min time points showed that there is a clear difference between the 3 kDa and the 10 kDa intensity profiles (Fig. 3C). Permeability coefficients of 3 and

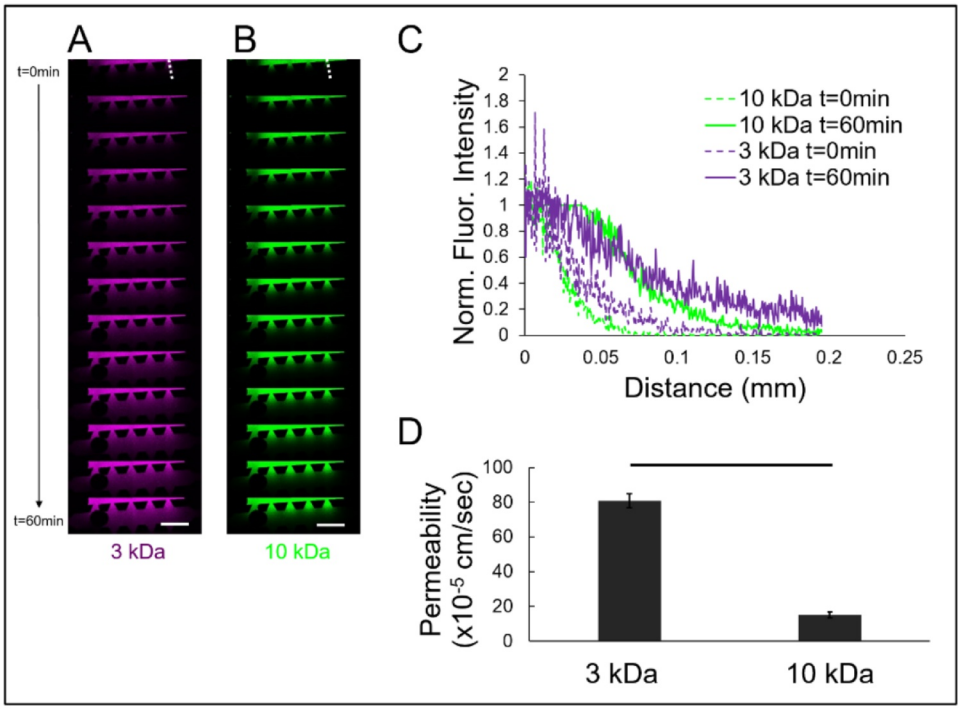

Fig. 3. Diffusion in LOC. Time lapse fluorescence images of (A) 3 kDa dextran in purple and (B) 10 kDa dextran in green. Time points are from 0 min. (top) to 60 min. (bottom). (C) Intensity profiles for 3 and 10 kDa dextran along the dashed lines in (A) and (B) for the 0 and 60 min. time points. (D) Permeability coefficients for 3 and 10 kDa. Mean ± s.e.m. were shown. Scale bars 1 mm. (For interpretation of the references to color in this figure legend, the reader is referred to the web version of this article.)

10 kDa dextran were 80.89 ± 4.07 and 15.10 ± 1.63 cm/sec, respectively, in agreement with previous studies (Kihara et al., 2013; Thomas et al., 2017; van Duinen et al., 2017; Frost et al., 2019). These results showed that the LOC devices allowed for diffusion of materials between the side and middle channels. Thus culture medium components can reach the cells embedded in the matrigel in the middle channel and support their viability. What is more, the molecular weights of DOX and KLA are 578.98 and 238.29 Da, respectively. These drugs are ~ 10-fold smaller than the 3 kDa dextran, and therefore, when loaded into the side channels, they can easily reach the cells in the middle channel.

3.2. Determination of the effect of drugs on the viability of cells in 3D monoculture in LOC devices

To confirm homogenous cell distribution in LOC devices, CellTracker Green stained MDA-MB-231 cells mixed 1:1 with matrigel were loaded into the middle channel of the LOC devices, side channels were loaded with culture medium and LOC devices were maintained in culture. Images of cells throughout the middle channel after 24 h showed that cells were distributed evenly in the middle channel (Fig. 4, Supplementary data Movie 2). 3D images at times indicated a slightly increased cell density towards the glass bottom of the LOC devices, possibly due to the fact that LOC devices were cultured with the glass part at the bottom side. Rotation during matrigel polymerization can therefore be preferred. Total cell density in LOC devices was 10 x 10^6 cells/ml resulting in an optimal apparent volumetric occupancy of 45 ± 4% of cells in matrigel.

To determine cell viability in monoculture in the presence and absence of drugs, MDA-MB-231 cells were first cultured in LOC devices for 24 h. Then, culture media in the side channels were replaced with fresh media containing DMSO, DOX or KLA. Culture was continued for another 48 h. Confocal imaging revealed the homogenous distribution of cells in the x-y plane was maintained throughout the 72 h of culture (Fig. 5, Supplementary data Movie 3, Fig. 7A). Dox was readily detected in the red channel because it has fluorescent property (Karukstis et al., 1998; Shah et al., 2017). Dead cells were detected in the far-red channel via NucRed Dead 647 staining. Cells treated with DMSO did not show significant signal in the far-red channel as expected (Fig. 5A, Fig. 7A). On the other hand, DOX and KLA treated cells showed prominent far-red signal (Fig. 5B, 5C, Fig. 7A). Quantification of images showed that the death index for DMSO, DOX and KLA were 0.022 ± 0.006, 0.225 ± 0.036 and 0.276 ± 0.016, respectively (Fig. 7A). The death indexes for DOX and KLA treated cells were significantly higher than that for DMSO treated cells, as expected ($p < 0.05$). Actually, the death indexes of DOX and KLA treated cells were 10 and 13 fold higher than that for DMSO treated cells. These results showed that KLA was as effective as DOX in killing MDA-MB-231 cells in 3D mono-culture in LOC devices; there was no statistically significant difference in the death indexes between DOX and KLA treated cells.

3.3. Determination of the effect of drugs on the viability of cells in 3D triculture in LOC devices

Cancer cells do not exist isolated *in vivo*. Therefore, determination of any effects of drugs on other cell types is crucial. Here, 3D tri-culture in LOC devices with and without drugs was performed. MDA-MB-231, MCF10A and RAW 264.7 cells were mixed at 1:1:1 ratio and then with matrigel before being loaded into the middle channel of LOC devices. Then side channels were loaded with culture medium. LOC devices were cultured for 24 h before the media in the side channels was replaced with fresh media containing DMSO, DOX or KLA and culture was continued for another 48 h. Using confocal fluorescence microscopy, MCF10A cells, MDA-MB-231 cells and all dead cells were detected in the blue, green and far-red channels, respectively. RAW264.7 cells were not labeled and thus were not visualized. Future work aims to include other stromal cell types and label all cells to better dissect drug effects.

3D images showed that the homogenous distribution of cells in the x-y-z volume was maintained throughout the 72 h of culture (Figs. 6, and 7B). As was the case in 3D mono-culture, DMSO treated cells did not show significant signal in the far-red channel corresponding to dead cells (Figs. 6A, and 7B) whereas DOX and KLA treated cells showed prominent far-red signal (Figs. 6B, 6C, 7B). To differentiate effects of DOX and KLA on MDA-231 and MCF10A cells, quantitative image analysis was carried out. The death indexes for DMSO, DOX and KLA treated MDA-MB-231 cells were 0.074 ± 0.021, 0.495 ± 0.018 and

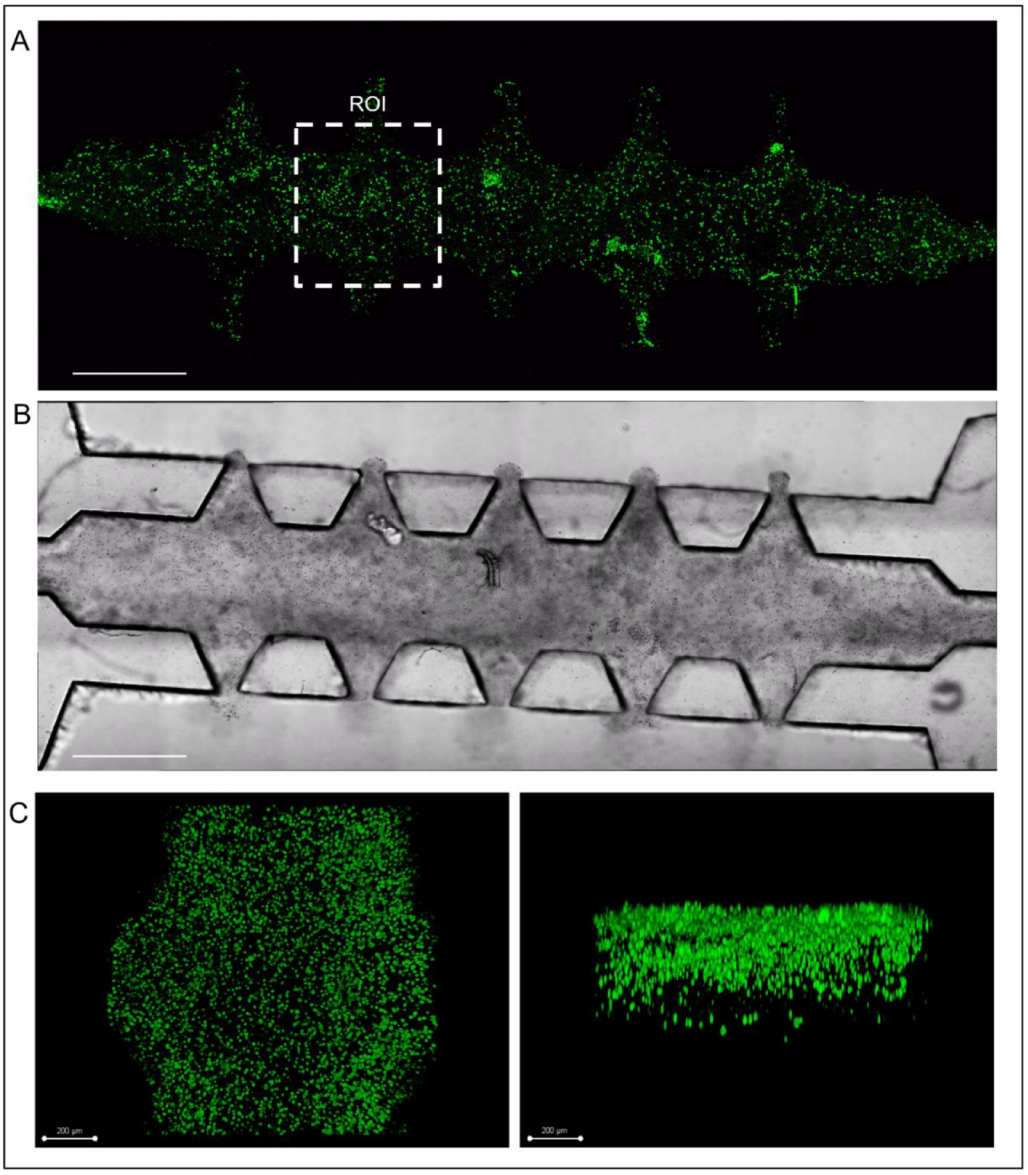

Fig. 4. (A) 2D Phase contrast image of LOC with MDA-MB-231 cells mixed with matrigel and loaded into the middle channel (time point: 24 h). (B) 2D image of CellTracker Green stained MDA-MB-231 cells in the same LOC. (C) 3D Top view of region of interest (ROI) in (A). (D) 3D Side view of ROI in (A). Scale bars 1 mm for (A) and (B), 200 µm for (C) and (D).

0.365 ± 0.016, respectively (Fig. 7B). The death indexes for DOX and KLA treated MDA-MB-231 cells in 3D tri-culture were both significantly higher than for DMSO treated cells ($p < 0.05$). Actually, the death indexes of DOX and KLA treated MDA-MB-231 cells were 7 and 5 fold higher than that of DMSO treated cells. Compared with KLA treated cells, DOX treated MDA-MB-231 cells had a 1.35-fold higher death index ($p < 0.05$) revealing that KLA caused 26% less cell death for MDA-MB-231 cells than DOX in 3D tri-culture in LOC devices.

The death indexes for DMSO, DOX and KLA treated MCF10A cells were 0.052 ± 0.013, 0.453 ± 0.022 and 0.201 ± 0.015, respectively (Fig. 6B). The death indexes for DOX and KLA treated MCF10A cells in 3D tri-culture were both significantly higher than for DMSO treated cells ($p < 0.05$). In fact, the death indexes of DOX and KLA treated MCF10A cells were 9 and 4 fold higher than that of DMSO treated cells. Compared with KLA treated cells, DOX treated MCF10A cells had a 2.25-fold higher death index ($p < 0.05$) revealing that KLA caused 56% less cell death for MCF10A cells than DOX in 3D tri-culture in LOC devices. The death index for DOX treated MCF10A and MDA-MB-231 cells were not statistically different in tri-culture, showing that DOX was not selective between cancer and normal mammary epithelial cells. On the other hand, the death index for KLA treated MDA-MB-231 cells was 1.81 fold higher than for MCF10A cells ($p < 0.05$), signifying that KLA was more effective on cancer cells. It is desired that anti-cancer drugs selectively act on cancer cells with minimum effects on other cells. In this regard, KLA is a promising anti-cancer drug candidate.

Comparing 3D mono- and tri-culture results revealed that the death index for DMSO treated MDA-MB-231 cells was higher in tri-culture ($p < 0.05$). In addition, both DOX and KLA induced 2.2 and 1.3 more cell death in MDA-MB-231 cells in tri-culture than in mono-culture, respectively ($p < 0.05$). In mono-culture models, cells do not reflect exactly the effect of drugs due to lack of stromal components in co-culture conditions (Brancato et al., 2018).The difference between mono- and tri-cultures observed here is probably due to the inter-cellular interactions in tri-culture conditions (Kawada et al., 1999; Betriu and Semino, 2018).

DOX is fluorescent, thus it is possible to quantify DOX uptake by cells. Image analysis revealed that DOX uptake indexes were

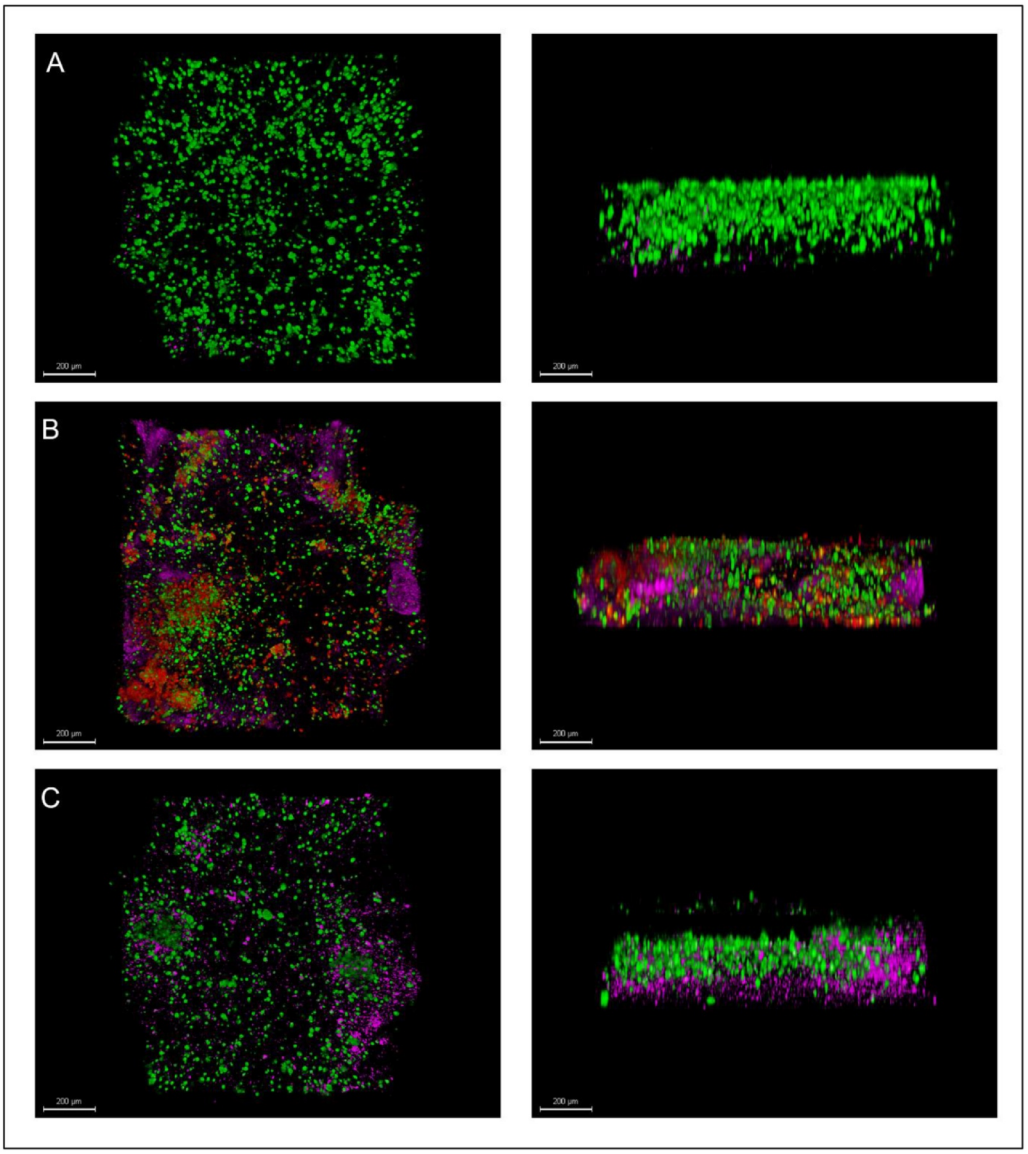

Fig. 5. Confocal fluorescence images of MDA-MB-231 cells treated with (A) DMSO, (B) DOX, (C) KLA. Images in the left and right showed top and side views, respectively. MDA-MB-231 cells, dead cells and DOX were shown in green, purple and red channels, respectively. Scale bars 200 µm. (For interpretation of the references to color in this figure legend, the reader is referred to the web version of this article.)

0.37 ± €0.046, 0.20 ± €0.006 and 0.39 ± €0.019, for MDA-MB-231 cells in mono-culture, MDA-MB-231 cells in tri-culture and MCF10A cells in tri-culture, respectively. MDA-MB-231 cells had 1.81 fold more DOX in mono-culture than they did in tri-culture ($p < 0.05$) probably due to the presence of other cells which also uptook DOX in tri-culture. Interestingly, DOX uptake by MCF10A cell was 1.96 fold higher than that by MDA-MB-231 cells in tri-culture ($p < 0.05$). This is expected, yet undesired, because cancer cells can transport intracellular drugs to the extracellular media and even acquire drug resistance (Tredan et al., 2007; Kibria et al., 2014; Au, et al., 2016; Moiseenko et al., 2017). Here, the death indexes between DOX treated MDA-MB-231 and MCF10A were not significantly different (Fig. 7B, 7C) showing that DOX was not selective. However, DOX can affect phenotypes in cells other than cell viability (Pilco-Ferreto and Calaf, 2016). Therefore, significantly more uptake of DOX by normal cells is likely to cause other unwanted effects than cell viability that was tested here (Davis et al., 2008; Demaria et al., 2017; Renu et al., 2018). These results are in agreement with *in vivo* studies for DOX. *In vivo* studies for KLA are a focus of future work and are expected to correlate with the results reached here. KLA is not a fluorescent molecule, and therefore its uptake by cells could not be studied. Future work can benefit from fluorescent conjugates of KLA.

Previous studies show that 3D cultures reflect the patient profile better than 2D cell cultures and different drug responses occur in 3D versus 2D cultures (Bonnier, et al., 2015; Casey et al., 2016). In addition, it is known that the effects of the drugs differ even between mono- and co-cultures. As the number of different cell types in the culture increases, the physiological relevance increases (Goers et al., 2014; Kasurinen et al., 2018). Furthermore, LOC devices enable local maxima for factors secreted from cells and better mimic the fluid/matrix to cell ratio observed *in vivo* (Paguirigan and Beebe, 2009). In the current study, the drug testing platform was based on 3D cell culture in LOC devices and mono- and tri-cultures were compared. Combination of 3D mono- and tri-culture results reveal that comparison of DOX and KLA is better performed in 3D tri-culture. In mono-culture, it was not possible to examine drug effects on other cells. What is more, effectiveness of drugs was different between mono- and tri- culture settings. 3D tri-culture is a better mimic of the *in vivo* conditions, and results of this study strongly recommend that 3D tri-culture rather than 3D mono-culture be used for drug testing.

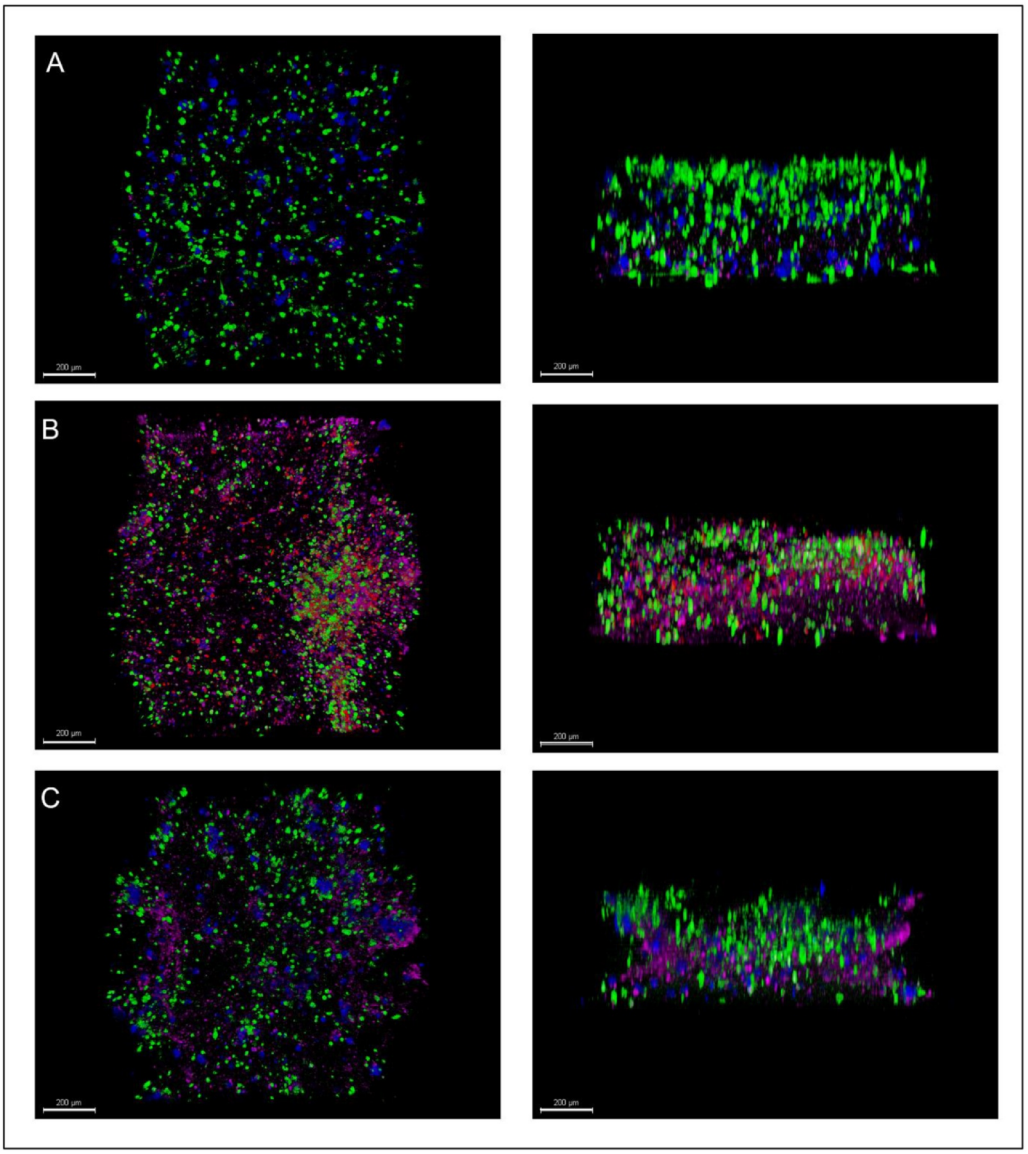

Fig. 6. Confocal fluorescence images of MDA-MB-231, MCF10A and RAW264.7 cells treated with (A) DMSO, (B) DOX, (C) KLA. Images in the left and right showed top and side views, respectively. MDA-MB-231 cells, MCF10A cells, dead cells and DOX were shown in green, blue, purple and red channels, respectively. RAW264.7 cells were not stained. Scale bars 200 µm. (For interpretation of the references to color in this figure legend, the reader is referred to the web version of this article.)

4. Conclusion

In this study, using a multidisciplinary approach, a new drug testing platform based on 3D tri-cultures in LOC devices was developed and used to compare two drugs, namely doxorubicin (DOX) and (*R*)-4′-methylklavuzon (KLA). Results showed that KLA was as effective as DOX in 3D mono-culture. While KLA resulted in 26% less cancer cell death than DOX in 3D tri-culture, the death index of KLA treated cancer cells was still 5 fold higher than untreated cancer cells. More importantly, KLA caused 56% less normal mammary epithelial cell death than DOX in 3D tri-culture showing that it is a promising, selective anti-cancer drug candidate. Collectively, the results clearly showed that cell culture conditions such as cellular diversity and dimensionality modulate effects of drugs.

The lack of adequate preclinical models is a major cause of the 90% failure rate in the drug discovery process. Therefore, development of platforms that can mimic the *in vivo* tissue microenvironment is an urgent need. This study developed, using a multidisciplinary approach, a platform based on 3D tri-culture in LOC devices. The platform provided physiologically relevant microenvironment and was able to realistically differentiate effects of drugs. Results strongly recommend that 3D tri-culture in LOC devices be used for assessment of drug toxicity at the preclinical stage.

The new platform can be used in future studies that perform high throughput comprehensive screens that include not-yet-characterized new molecules.

CRediT authorship contribution statement

Begum Gokce: Data curation, Formal analysis, Visualization, Writing - original draft. **Ismail Akcok:** Resources. **Ali Cagir:** Writing - review & editing, Funding acquisition. **Devrim Pesen-Okvur:** Conceptualization, Methodology, Formal analysis, Visualization, Writing - review & editing, Supervision, Funding acquisition.

Acknowledgements

This work was supported by Turkish Academy of Sciences – The Young Scientists Award 2016, The Science Academy Society of Turkey – Young Scientists Award 2016 and Izmir Institute of Technology –

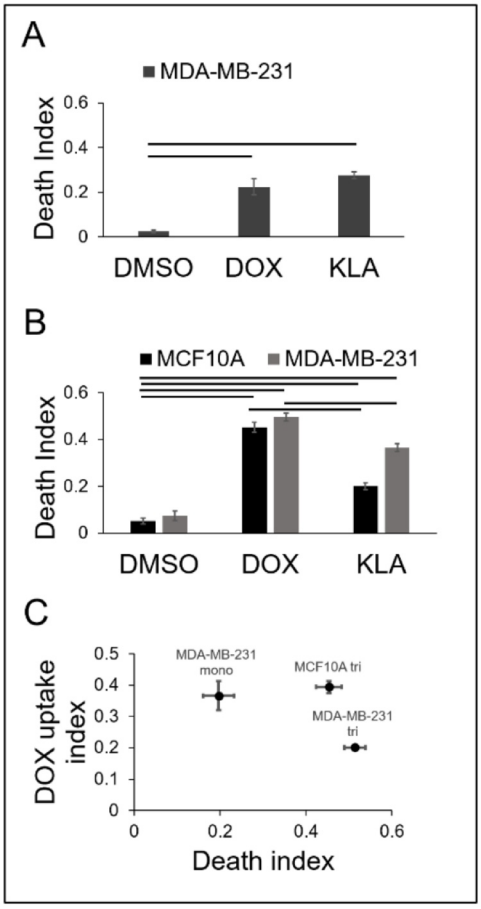

Fig. 7. Death and DOX uptake indexes. (A) Death index of MDA-MB-231 cells in mono-culture treated with DMSO, DOX and KLA. (A) Death index of MDA-MB-231 and MCF10A cells in tri-culture treated with DMSO, DOX and KLA. (C) DOX uptake index vs. death index for MDA-MB-231 in mono- and tri- as well as MCF10A cells in tri-culture treated with DOX. Mean ± s.e.m. were shown. Horizontal bars showed statistically significant differences.

2017G_IYTE97 research grants awarded to Devrim Pesen Okvur. Samples were fabricated in the IYTE Applied Quantum Research Center, supported by State Planning Organization – Grant 2009K120860. Synthesis was supported by the Scientific and Technological Research Council of Turkey – TUBITAK 110T782 grant to Ali Cagir. We thank Katherine Willcox Ozsari from Izmir Institute of Technology Academic Writing Center for assisting in English language editing.

Supplementary materials

Supplementary material associated with this article can be found, in the online version, at doi:10.1016/j.ejps.2020.105542.

References

Akcok, I., Mete, D., Sen, A., Kasaplar, P., Korkmaz, K.S., Cagir, A., 2017. Synthesis and topoisomerase I inhibitory properties of klavuzon derivatives. Bioorg. Chem. 71, 275–284.

Alterovitz, G., Dean, D., Goble, C., Crusoe, M.R., Soiland-Reyes, S., Bell, A., Hayes, A., Suresh, A., Purkayastha, A., King, C.H., Taylor, D., Johanson, E., Thompson, E.E., Donaldson, E., Morizono, H., Tsang, H., Vora, J.K., Goecks, J., Yao, J., Almeida, J.S., Keeney, J., Addepalli, K., Krampis, K., Smith, K.M., Guo, L., Walderhaug, M., Schito, M., Ezewudo, M., Guimera, N., Walsh, P., Kahsay, R., Gottipati, S., Rodwell, T.C., Bloom, T., Lai, Y., Simonyan, V., Mazumder, R., 2018. Enabling precision medicine via standard communication of HTS provenance, analysis, and results. PLoS Biol. 16 (12), e3000099.

Amelian, A., Wasilewska, K., Megias, D., Winnicka, K., 2017. Application of standard cell cultures and 3D in vitro tissue models as an effective tool in drug design and development. Pharmacol. Rep. 69 (5), 861–870.

Arcamone, F., Cassinelli, G., Fantini, G., Grein, A., Orezzi, P., Pol, C., Spalla, C., 1969. Adriamycin, 14-hydroxydaunomycin, a new antitumor antibiotic from S. peucetius var. caesius. Biotechnol. Bioeng. 11 (6), 1101–1110.

Au, J.L., Yeung, B.Z., Wientjes, M.G., Lu, Z., Wientjes, M.G., 2016. Delivery of cancer therapeutics to extracellular and intracellular targets: Determinants, barriers, challenges and opportunities. Adv. Drug. Deliv. Rev. 97, 280–301.

Barata, D., van Blitterswijk, C., Habibovic, P., 2016. High-throughput screening approaches and combinatorial development of biomaterials using microfluidics. Acta Biomater. 34, 1–20.

Betriu, N., Semino, C.E., 2018. Development of a 3D co-culture system as a cancer model using a self-assembling peptide scaffold. Gels 4 (3).

Bhatia, S.N., Ingber, D.E., 2014. Microfluidic organs-on-chips. Nat. Biotechnol. 32 (8), 760–772.

Bonnier, F., Keating, M.E., Wrobel, T.P., Majzner, K., Baranska, M., Garcia-Munoz, A., Blanco, A., Byrne, H.J., 2015. Cell viability assessment using the Alamar blue assay: a comparison of 2D and 3D cell culture models. Toxicol. Vitro 29 (1), 124–131.

Brancato, V., Gioiella, F., Imparato, G., Guarnieri, D., Urciuolo, F., Netti, P.A., 2018. 3D breast cancer microtissue reveals the role of tumor microenvironment on the transport and efficacy of free-doxorubicin in vitro. Acta Biomater. 75, 200–212.

Brenner, J., Brenner, H.J., 1983. [The treatment of cancer by anthracyclines]. Harefuah 104 (5), 205–207.

Casey, A., Gargotti, M., Bonnier, F., Byrne, H.J., 2016. Chemotherapeutic efficiency of drugs in vitro: comparison of doxorubicin exposure in 3D and 2D culture matrices. Toxicol. Vitro 33, 99–104.

Cukierman, E., Pankov, R., Stevens, D.R., Yamada, K.M., 2001. Taking cell-matrix adhesions to the third dimension. Science 294 (5547), 1708–1712.

Davis, M.E., Chen, Z., Shin, D.M., 2008. Nanoparticle therapeutics: an emerging treatment modality for cancer. Nat. Rev. Drug Discov. 7 (9), 771–782.

Delman, M., Avcı, S.T., Akçok, İ., Kanbur, T., Erdal, E., Çağır, A., 2019. Antiproliferative activity of (R)-4′-methylklavuzon on hepatocellular carcinoma cells and EpCAM +/CD133+ cancer stem cells via SIRT1 and Exportin-1 (CRM1) inhibition. Eur. J. Med. Chem. 180, 224–237.

Demaria, M., O'Leary, M.N., Chang, J.H., Shao, L.J., Liu, S., Alimirah, F., Koenig, K., Le, C., Mitin, N., Deal, A.M., Alston, S., Academia, E.C., Kilmarx, S., Valdovinos, A., Wang, B.S., de Bruin, A., Kennedy, B.K., Melov, S., Zhou, D.H., Sharpless, N.E., Muss, H., Campisi, J., 2017. Cellular senescence promotes adverse effects of chemotherapy and cancer relapse. Cancer Discov. 7 (2), 165–176.

Duval, K., Grover, H., Han, L.H., Mou, Y., Pegoraro, A.F., Fredberg, J., Chen, Z., 2017. Modeling physiological events in 2D vs. 3D cell culture. Physiology (Bethesda). 32 (4), 266–277.

Edmondson, R., Broglie, J.J., Adcock, A.F., Yang, L.J., 2014. Three-dimensional cell culture systems and their applications in drug discovery and cell-based biosensors. Assay Drug Dev. Technol. 12 (4), 207–218.

Farooq, U., Haider, Z., Liang, X.M., Memon, K., Hossain, S.M.C., Zheng, Y., Xu, H.S., Qadir, A., Panhwar, F., Dong, S.R., Zhao, G., Luo, J.K., 2019. Surface-acoustic-wave-based lab-on-chip for rapid transport of cryoprotectants across cell membrane for cryopreservation with significantly improved cell viability. Small 15 (14).

Frost, T.S., Jiang, L., Lynch, R.M., Zohar, Y., 2019. Permeability of epithelial/endothelial barriers in transwells and microfluidic bilayer devices. Micromachines (Basel) 10 (8).

Goers, L., Freemont, P., Polizzi, K.M., 2014. Co-culture systems and technologies: taking synthetic biology to the next level. J. R. Soc. Interface 11 (96).

Hirschhaeuser, F., Menne, H., Dittfeld, C., West, J., Mueller-Klieser, W., Kunz-Schughart, L.A., 2010. Multicellular tumor spheroids: An underestimated tool is catching up again. J. Biotechnol. 148 (1), 3–15.

Huh, D., Hamilton, G.A., Ingber, D.E., 2011. From 3D cell culture to organs-on-chips. Trends Cell Biol. 21 (12), 745–754.

Imamura, Y., Mukohara, T., Shimono, Y., Funakoshi, Y., Chayahara, N., Toyoda, M., Kiyota, N., Takao, S., Kono, S., Nakatsura, T., Minami, H., 2015. Comparison of 2D- and 3D-culture models as drug-testing platforms in breast cancer. Oncol. Rep. 33 (4), 1837–1843.

Kanbur, T., Kara, M., Kutluer, M., Sen, A., Delman, M., Alkan, A., Otas, H.O., Akcok, I., Cagir, A., 2017. CRM1 inhibitory and antiproliferative activities of novel 4′-alkyl substituted klavuzon derivatives. Bioorg. Med. Chem. 25 (16), 4444–4451.

Karukstis, K.K., Thompson, E.H., Whiles, J.A., Rosenfeld, R.J., 1998. Deciphering the fluorescence signature of daunomycin and doxorubicin. Biophys. Chem. 73 (3), 249–263.

Kasaplar, P., Yilmazer, O., Cagir, A., 2009. 6-Bicycloaryl substituted (S)- and (R)-5,6-dihydro-2H-pyran-2-ones: asymmetric synthesis, and anti-proliferative properties. Bioorg. Med. Chem. 17 (1), 311–318.

Kasurinen, S., Happo, M.S., Ronkko, T.J., Orasche, J., Jokiniemi, J., Kortelainen, M., Tissari, J., Zimmermann, R., Hirvonen, M.R., Jalava, P.I., 2018. Differences between co-cultures and monocultures in testing the toxicity of particulate matter derived from log wood and pellet combustion. PLoS One 13 (2), e0192453.

Kawada, M., Ishizuka, M., Takeuchi, T., 1999. Enhancement of antiproliferative effects of interleukin-1beta and tumor necrosis factor-alpha on human prostate cancer LNCaP cells by coculture with normal fibroblasts through secreted interleukin-6. Jpn. J. Cancer Res. 90 (5), 546–554.

Keizer, H.G., Pinedo, H.M., Schuurhuis, G.J., Joenje, H., 1990. Doxorubicin (adriamycin) - a critical-review of free radical-dependent mechanisms of cytotoxicity. Pharmacol. Ther. 47 (2), 219–231.

Khajuria, D.K., Vasireddi, R., Priydarshi, M.K., Mahapatra, D.R., 2020. Ionic diffusion and drug release behavior of core-shell-functionalized alginate-chitosan-based hydrogel. ACS Omega 5 (1), 758–765.

Kibria, G., Hatakeyama, H., Akiyama, K., Hida, K., Harashima, H., 2014. Comparative study of the sensitivities of cancer cells to doxorubicin, and relationships between the effect of the drug-efflux pump P-gp. Biol. Pharm. Bull. 37 (12), 1926–1935.

Kihara, T., Ito, J., Miyake, J., 2013. Measurement of biomolecular diffusion in extracellular matrix condensed by fibroblasts using fluorescence correlation spectroscopy. PLoS One 8 (11), e82382.
Ma, H., Liu, T., Qin, J., Lin, B., 2010. Characterization of the interaction between fibroblasts and tumor cells on a microfluidic co-culture device. Electrophoresis 31 (10), 1599–1605.
Miki, Y., Ono, K., Hata, S., Suzuki, T., Kumamoto, H., Sasano, H., 2012. The advantages of co-culture over mono cell culture in simulating in vivo environment. J. Steroid Biochem. Mol. Biol. 131 (3-5), 68–75.
Moiseenko, F., N. Volkov, A. Bogdanov, M. Dubina and V. Moiseyenko (2017). "Resistance mechanisms to drug therapy in breast cancer and other solid tumors: An opinion." F1000 Res6: 288.
Namer, M., 1993. Anthracyclines in the adjuvant treatment of breast cancer. Drugs 45 (Suppl 2), 4–9.
Oliveira, N.M., Vilabril, S., Oliveira, M.B., Reis, R.L., Mano, J.F., 2019. Recent advances on open fluidic systems for biomedical applications: A review. Mater. Sci. Eng. C Mater. Biol. Appl. 97, 851–863.
Ozdil, B., Onal, S., Oruc, T., Pesen Okvur, D., 2014. Fabrication of 3D controlled in vitro microenvironments. MethodsX 1, 60–66.
Paguirigan, A.L., Beebe, D.J., 2009. From the cellular perspective: exploring differences in the cellular baseline in macroscale and microfluidic cultures. Integr. Biol. (Camb) 1 (2), 182–195.
Pilco-Ferreto, N., Calaf, G.M., 2016. Influence of doxorubicin on apoptosis and oxidative stress in breast cancer cell lines. Int. J. Oncol. 49 (2), 753–762.
Popova, A.A., Schillo, S.M., Demir, K., Ueda, E., Nesterov-Mueller, A., Levkin, P.A., 2015. Droplet-Array (DA) sandwich chip: a versatile platform for high-throughput cell screening based on superhydrophobic-superhydrophilic micropatterning. Adv. Mater. 27 (35), 5217–5222.
Renu, K., Abilash, V.G., Pichiah, P.B.T., Arunachalam, S., 2018. Molecular mechanism of doxorubicin-induced cardiomyopathy - An update. Eur. J. Pharmacol. 818, 241–253.
Schindelin, J., Arganda-Carreras, I., Frise, E., Kaynig, V., Longair, M., Pietzsch, T., Preibisch, S., Rueden, C., Saalfeld, S., Schmid, B., Tinevez, J.Y., White, D.J., Hartenstein, V., Eliceiri, K., Tomancak, P., Cardona, A., 2012. Fiji: an open-source platform for biological-image analysis. Nat. Methods 9 (7), 676–682.
Schneider, C.A., Rasband, W.S., Eliceiri, K.W., 2012. NIH Image to ImageJ: 25 years of image analysis. Nat. Methods 9 (7), 671–675.
Schuhmacher, A., Gassmann, O., McCracken, N., Hinder, M., 2018. Open innovation and external sources of innovation. An opportunity to fuel the R&D pipeline and enhance decision making? J. Transl. Med. 16 (1), 119.
Shah, S., Chandra, A., Kaur, A., Sabnis, N., Lacko, A., Gryczynski, Z., Fudala, R., Gryczynski, I., 2017. Fluorescence properties of doxorubicin in PBS buffer and PVA films. J. Photochem. Photobiol. B 170, 65–69.
Shield, K., Ackland, M.L., Ahmed, N., Rice, G.E., 2009. Multicellular spheroids in ovarian cancer metastases: Biology and pathology. Gynecol. Oncol. 113 (1), 143–148.
Tacar, O., Indumathy, S., Tan, M.L., Baindur-Hudson, S., Friedhuber, A.M., Dass, C.R., 2015. Cardiomyocyte apoptosis vs autophagy with prolonged doxorubicin treatment: comparison with osteosarcoma cells. J. Pharm. Pharmacol. 67 (2), 231–243.
Tacar, O., Sriamornsak, P., Dass, C.R., 2013. Doxorubicin: an update on anticancer molecular action, toxicity and novel drug delivery systems. J. Pharm. Pharmacol. 65 (2), 157–170.
Thomas, A., Wang, S., Sohrabi, S., Orr, C., He, R., Shi, W., Liu, Y., 2017. Characterization of vascular permeability using a biomimetic microfluidic blood vessel model. Biomicrofluidics 11 (2), 024102.
Tredan, O., Galmarini, C.M., Patel, K., Tannock, I.F., 2007. Drug resistance and the solid tumor microenvironment. J. Natl. Cancer Inst. 99 (19), 1441–1454.
van Duinen, V., van den Heuvel, A., Trietsch, S.J., Lanz, H.L., van Gils, J.M., van Zonneveld, A.J., Vulto, P., Hankemeier, T., 2017. 96 perfusable blood vessels to study vascular permeability in vitro. Sci. Rep. 7 (1), 18071.
Wang, S.W., Konorev, E.A., Kotamraju, S., Joseph, J., Kalivendi, S., Kalyanaraman, B., 2004. Doxorubicin induces apoptosis in normal and tumor cells via distinctly different mechanisms - Intermediacy of H2O2- and p53-dependent pathways. J. Biol. Chem. 279 (24), 25535–25543.
Waters, R. (2019). World Preview 2019, Outlook to 2024. L. Urquhart.
Wielhouwer, E.M., Ali, S., Al-Afandi, A., Blom, M.T., Riekerink, M.B.O., Poelma, C., Westerweel, J., Oonk, J., Vrouwe, E.X., Buesink, W., vanMil, H.G.J., Chicken, J., van't Oever, R., Richardson, M.K., 2011. Zebrafish embryo development in a microfluidic flow-through system. Lab. Chip 11 (10), 1815–1824.
Wong, H.L., Bendayan, R., Rauth, A.M., Xue, H.Y., Babakhanian, K., Wu, X.Y., 2006. A mechanistic study of enhanced doxorubicin uptake and retention in multidrug resistant breast cancer cells using a polymer-lipid hybrid nanoparticle system. J. Pharmacol. Exp. Ther. 317 (3), 1372–1381.
Woodcock, J., Woosley, R., 2008. The FDA critical path initiative and its influence on new drug development. Annu. Rev. Med. 59, 1–12.
Yanagisawa, A., Kageyama, H., Nakatsuka, Y., Asakawa, K., Matsumoto, Y., Yamamoto, H., 1999. Enantioselective addition of allylic trimethoxysilanes to aldehydes catalyzed by p-Tol-BINAP.AgF. Angew. Chem.-Int. Edition 38 (24), 3701–3703.
Yildirim, E., Trietsch, S.J., Joore, J., van den Berg, A., Hankemeier, T., Vulto, P., 2014. Phaseguides as tunable passive microvalves for liquid routing in complex microfluidic networks. Lab Chip 14 (17), 3334–3340.
Ziolkowska, K., Kwapiszewski, R., Brzozka, Z., 2011. Microfluidic devices as tools for mimicking the in vivo environment. New J. Chem. 35 (5), 979–990.